USING HIGH-SPEED VIDEO TO BETTER UNDERSTAND EXTENDED COLUMN TESTS

Karl W. Birkeland[1,*] and Alec van Herwijnen[2]

[1] USDA Forest Service National Avalanche Center, Bozeman, Montana, USA
[2] WSL Swiss Federal Institute for Snow and Avalanche Research SLF, Davos, Switzerland

Abstract: Extended Column Tests (ECTs) have become increasingly popular for assessing snowpack stability. However, we still do not fully understand what happens to the block and the underlying weak layer during the test. Such work has been done for the Propagation Saw Test (PST), but not for the ECT. In order to better understand and interpret ECT results, we analyzed high-speed video (240 frames/second) of propagating ECTs using particle tracking. Our results show several things: 1) fractures initiate in an area of the weak layer directly under the shovel at the free edge of the block, 2) at the resolution of our measurements we do not see signs of progressive damage accumulation in the weak layer during tapping, but rather a single rapid collapse when fracture is initiated, 3) tapping on one side of the ECT does not affect the far side of the ECT, and 4) measured fracture speeds are similar to previously reported values, including those measured using the PST. From a practical perspective, our results suggest that the ECT is indeed measuring the propensity of a crack to propagate at the small scale of the ECT block, giving us greater confidence that we are capturing a critically important property of snow stability in our tests.

1. INTRODUCTION

The Extended Column Test (ECT) is a relatively new snowpack stability test, involving isolating a block 90 cm cross-slope by 30 cm upslope and then progressively loading one side of the block similar to a compression test [*Simenhois and Birkeland*, 2006; 2009]. The avalanche community rapidly adopted the ECT since its introduction, making it the most popular stability test conducted by SnowPilot users [*Birkeland and Chabot*, In press]. It has been studied in several different snow climates and countries [*Moner et al.*, 2008; *Ross and Jamieson*, 2008; *Winkler and Schweizer*, 2009]. However, so far all the work on the ECT has focused on its usefulness for predicting avalanche conditions rather than what happens mechanically during the test.

The Propagation Saw Test (PST) is another new test [*Gauthier and Jamieson*, 2006; 2008]. This test involves isolating a block that is 30 cm cross-slope by 100 cm (or twice the slab depth, whichever is greater) upslope and then cutting the weak layer with a snow saw until the introduced crack propagates. The PST has also gained a following amongst people evaluating avalanche conditions, and was the third most common field test in the SnowPilot database this past season [*Birkeland and Chabot*, In press]. In contrast to the ECT, the PST has been the subject of numerous studies focusing on the mechanics during the test, and researchers have used the results of such work to better understand some of the fundamental processes during fracture [*Bair et al.*, 2012; *Schweizer et al.*, 2011; *van Herwijnen and Heierli*, 2009; 2010; *van Herwijnen et al.*, 2010]. Much of this latter work utilizes particle tracking, where the observer inserts markers into the snowpack and then conducts tests while filming with a high speed video camera. The video can later be analyzed and very small movements in the markers can be tracked.

In this paper we apply the same particle tracking techniques used for the PST studies to the ECT. Our goal is to better understand what happens during a test, such as whether or not the whole block is being affected by the tapping, where the fracture initiates, and whether fracture speeds in the ECT are similar to those measured with the PST. An improved mechanical understanding of the test will help us to better interpret test results and their potential limitations.

2. METHODS

2.1 Data collection

We collected data at seven sites during the 2011/12 winter in southwest Montana, U.S.A (Table 1). Data collection involved travelling into the field on days when crack propagation was

[*] *Corresponding author address:* Karl Birkeland, USDA Forest Service National Avalanche Center, P.O. Box 130, Bozeman, MT 59771, tel: 406-587-6954, email: kbirkeland@fs.fed.

Table 1: Overview of the snow properties at each field site. The number of experiments (N), slope angle (θ), weak layer grain form (F), slab depth (H) and mean slab density (ρ_{slab}) are shown for each site.

Site	*N*	*θ*	*F*	*H* (cm)	ρ_{slab} (kg m^{-3})
A	5	35	DH	39	194
B	2	25	SH	37	190
C	1	36	FC	53	316
D	5	30	SH	43	143
E	2	24	SH	67	180
F	3	22	SH	35	169
G	2	10	SH	32	248

likely, as evidenced by ECTP results. At each field site we collected a manual snow profile and conducted one or several ECTs according to the procedure outlined in *Greene et al.* [2010]. In many cases we used wider columns to allow us to better evaluate what occurs during fracture at distances farther from the tapping area (Figure 1a). After ECT preparation, we inserted black plastic markers into the pit wall. Then we set up a camera on a tripod pointing directly at the pit wall. During the test we stood off to the side while doing the tapping so that all the markers were visible to the camera.

One difficulty was that if we tapped on the block too hard or if the snow was very soft, snow fell in front of some of the markers and markers fell out of the pit wall as the block was crushed (Figure 1b). This made it difficult, or in some cases impossible, to accurately track the markers immediately below the shovel. This problem did not affect areas further away from the shovel. To mitigate for the falling snow, we later attempted to insert a piece of cardboard to protect those lower discs from the falling snow, with limited success.

2.2 Data analysis

We utilized a particle tracking velocimetry (PTV) algorithm to analyze the motion of the markers [*Crocker and Grier*, 1996]. Coordinates are assigned to the centroid of each marker by using a spatial band pass filter to search for a local brightness minima. In this way, the position of the markers in each video frame can be determined with a mean accuracy of 0.1 mm. The accuracy of the particle tracking software depends on the size and the quality of the images, i.e. signal-to-noise ratio. By connecting the dots, the trajectories of the markers were determined during the entire test.

The displacement of a marker in the horizontal direction u_x and in the vertical direction u_z was defined as the displacement relative to the initial position, that is, the average position of the marker prior to movement. For propagating cracks, there is a delay between the vertical displacement of subsequent markers. The time delay between the onset of movement between markers is

a) 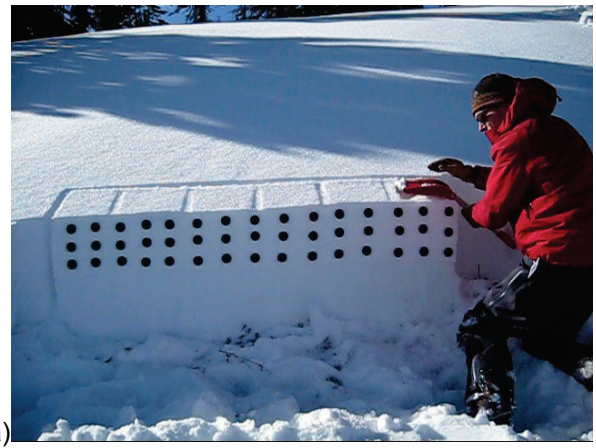 b) 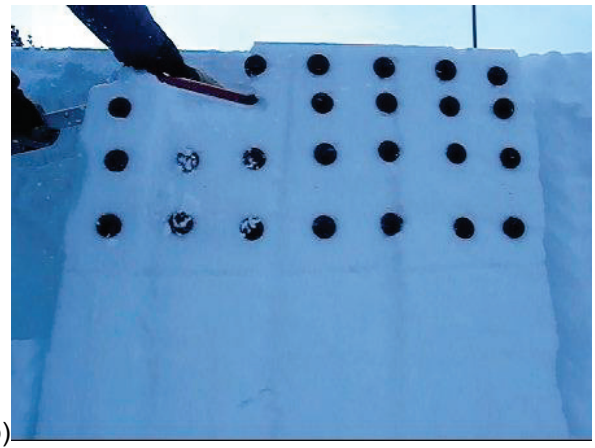

Figure 1: a) The experimental setup consisted of taking high speed videos of ECTs with black makers inserted into the pit wall, b) When the blocks needed to be tapped from the elbow or shoulder to fracture, falling snow partially obscured discs directly under the shovel, making tracking those discs difficult or impossible. We later utilized a piece of cardboard to capture falling snow so that these data could be analyzed, with limited success.

proportional to the distance between the markers and was used to calculate the propagation speed *c* of the fracture [*van Herwijnen and Jamieson*, 2005].

3. RESULTS AND DISCUSSION

We analyzed the deformation of the slab during 20 ECT's at seven different sites with slope angles (θ) ranging from 10 to 35 degrees (Table 1). The majority of weak layers consisted of buried surface hoar (SH), while one weak layer consisted of depth hoar (DH) and one of faceted grains (FC). We tested a variety of slabs, consisting of soft new snow (D), soft faceted snow (A, D and G), rounded snow (B and E) and wind deposited snow (C). Slab depth ranged from 32 to 67 cm and mean slab density ranged from 143 to 316 kg m^{-3}.

Tapping on the block mainly compacted the snow directly below the snow shovel and had little influence deeper in the snow cover or further away from the shovel. For example, during the ECT the snow column in test E1 was considerably compressed (Figure 2a and 2b). The displacement of markers in the upper half of the slab directly below the shovel therefore exhibited the largest displacements (dark and light blue curves in Figure 2c and 2d). On the other hand, the displacement of markers closer to the weak layer and further away from the shovel (green, yellow, orange and red curves in Figure 2c and 2d) was negligible up to weak layer fracture. Note that the displacements observed after each tap (indicated with the dashed lines in Figure 2c and 2d) resulted from snow falling in front of the markers. Some preliminary work has been conducted utilizing capacitive sensors to measure stress, and this work also shows that ECT tapping does not affect the far side of the block [*S. Thumlert, pers. comm.*, 2011].

Displacements of the markers closest to the weak layer in all our ECTPs were negligible up to weak layer fracture. This is clearly shown for a row of markers directly above the weak layer in test B1 in Figure 3a. These results also show that weak layer fracture starts at the free end of the column and propagates to the far end of the column. Fluctuations in the total vertical displacement after weak layer collapse seen in Figure 3a are also commonly observed in PSTs [e.g., *van Herwijnen et al.,* 2010], and likely relate to small scale changes in microstructural properties of the weak layer. In some ECTNs, on the other hand, we observed a gradual collapse of the weak layer after each tap, as seen in Figure 3b for test F2. Overall, our results suggest that there is no gradual damage accumulation in the weak layer during tapping in an ECT before weak layer fracture. However, if the fracture arrests before crossing the entire column, subsequent tapping can result in further compaction of the weak layer.

Table 2: Overview of ECT results and particle tracking velocimetry (PTV) measurements. ECT results are shown according to Greene et al. (2010): ECTP## - fracture initiates and propagates across the entire column on tap ##; ECTN## - fracture initiates without full propagation on tap ##. PTV measurement accuracy (ε), the range of vertical displacement in the area where the weak layer fractured (Δy) and fracture speeds (c) are also shown.

Test	Test result	ε (mm)	Δy (mm)	c (m s^{-1})
A1	ECTP 12[a]	0.2	~	20±2
A2	ECTN 18	0.3	~	~
A3	ECTN 11	0.3	6.5-2.3	~
A4	ECTP 22[a]	0.2	~	22±5
A5	ECTP 16[a]	0.05	~	17±2
B1	ECTP 3	0.06	6.4-3.7	13±1
B2	ECTP 7	0.1	6.6-2.1	14±1
C1	ECTP 17[a]	0.1	~	45±3
D1	ECTN 19	0.1	12.7-4.7	~
D2	ECTN 20[b]	0.2	1.5-0.7	~
D3	ECTP 21	0.2	9.9-5.1	16±1
D4	ECTP 25	0.1	10.6-5.3	19±2
D5	ECTP 23	0.2	9.3-4.9	15±2
E1	ECTN 17[b]	0.1	19.4-1.2	~
E2	ECTN 17[b]	0.05	12.5-4.3	~
F1	ECTP 11	0.06	4.4-0.5	10±1
F2	ECTN 15[b]	0.03	1.6-0.04	~
F3	ECTN 11[b]	0.03	4.6-0.05	~
G1	ECTN 16	0.06	11.6-0.7	~
G2	ECTN 18	0.03	3.8-1.7	~

[a] the column slid down-slope after fracture
[b] the fracture propagated beyond the area below the shovel but not across the entire column

Fracture speeds in our ECTP tests ranged from 10 to 45 m s^{-1}, with most speeds between 14 and 22 m s^{-1} (Table 2). Though the range of our measurements is large, they are in good agreement with measurements by *Johnson et al.* [2004], *van Herwijnen* [2005], and *van Herwijnen et al.* [2010] (Figure 4). Interestingly, when we combine the data from this study with previous work, we find a statistically significant relationship

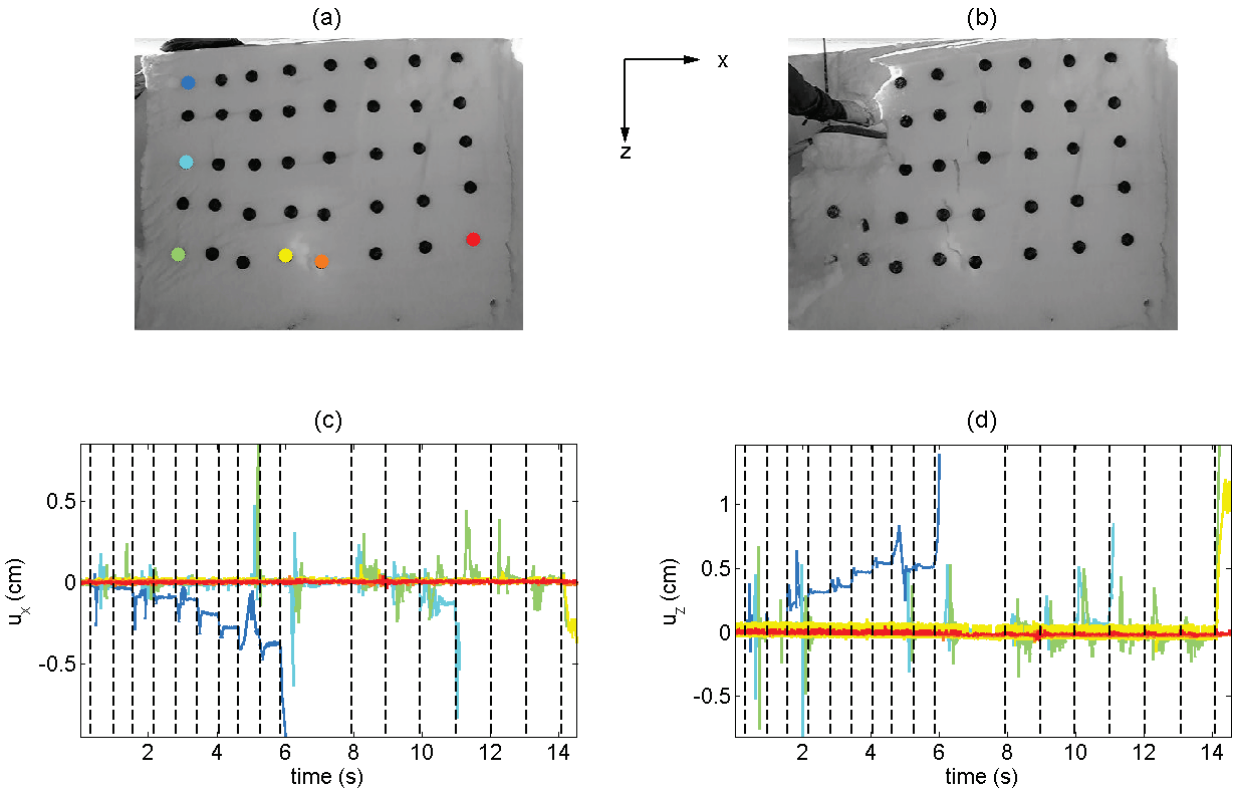

Figure 2: Results from experiment E1, which had a result of ECTN 17. (a) Image taken at the start of the test. The colored dots show the markers for which the displacements are shown. (b) Image taken at the end of the test showing considerable crushing of the column and partial weak layer fracture. (c) Horizontal displacement with time. (d) Vertical displacement with time. The colors of the displacement curves correspond to the markers indicated with the colored dots in (a). The dashed lines correspond to taps.

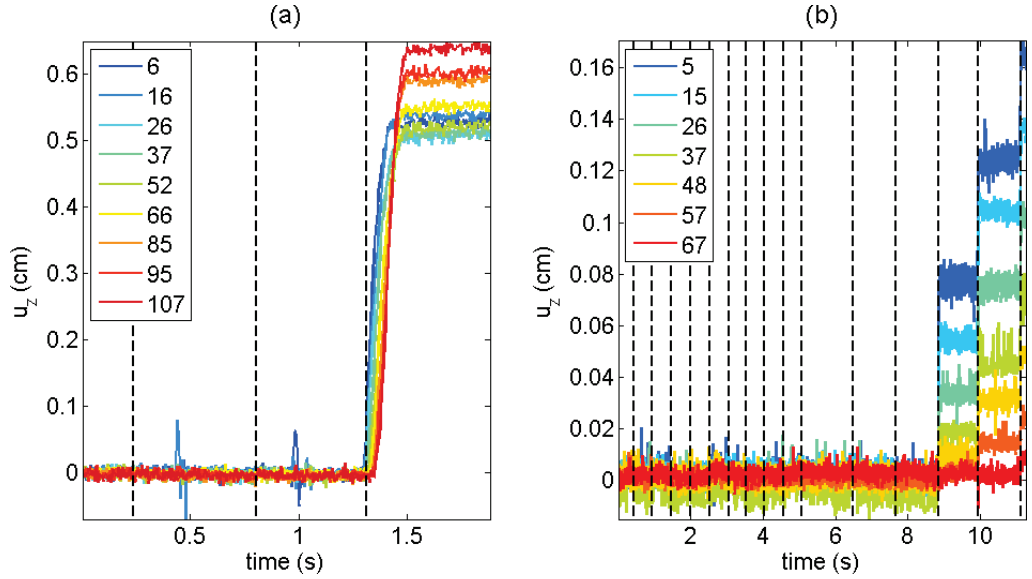

Figure 3: Vertical displacement with time for the row of marker closest to the weak layer in tests (a) B1 (ECTP 3) and (b) F2 (ECTN 15). The colors of the lines correspond to the distance of the center of the markers to the free edge of the column in cm, as indicated in the legend.

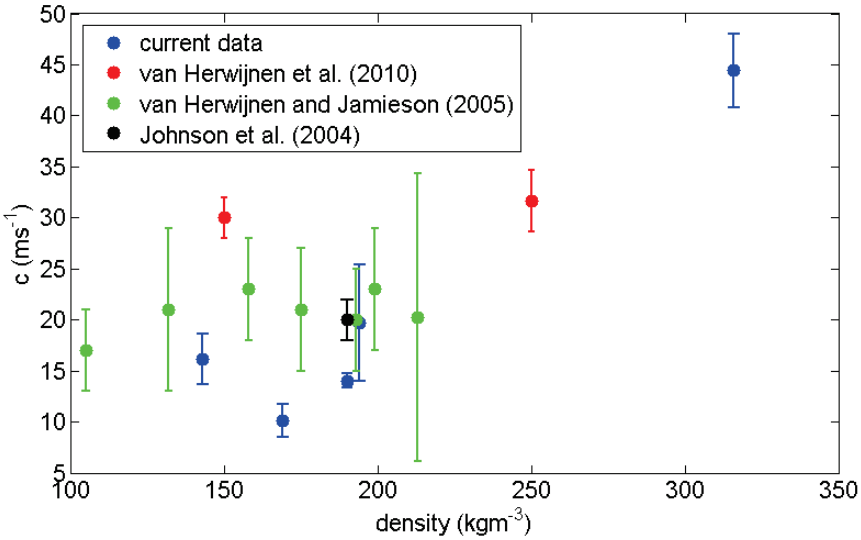

Figure 4: Fracture speed with slab density. Data from this study are shown, as well as data from van Herwijnen et al. *[2010],* van Herwijnen and Jamieson *[2005], and* Johnson et al. *[2004].*

between fracture speed and slab density (Pearson $r = 0.7$, $p = 2 \times 10^{-4}$). Despite our relatively short columns, we observed changes in propagation speeds with distance (not shown). Changes in *c* were relatively small in the ECTPs and no consistent trend was observed. Fracture speeds increased (A4, A5, B1, B2 and D3), stayed relatively constant (C1 and D5), or decreased (A1, D4 and F1). This is in line with results presented by van Herwijnen et al. (2010), who found no consistent trend in propagations speeds in much longer PSTs. All in all, our observations on crack propagation in ECTPs are consistent with results obtained from PSTs, increasing our confidence that the ECT provides valuable insight into weak layer crack propagation.

4. CONCLUSIONS

Using particle tracking velocimetry, we analyzed the displacement of the snow slab during 20 ECTs at seven different sites. Though the ECT is widely used, previously we did not know exactly what happens to the slab and weak layer during the test. Our results partially fill this gap, providing a better understanding of the mechanics of the ECT. Our results lead to some important conclusions:

- Tapping only affects the snow immediately below the shovel and does not affect the far end of the column. This suggests that the ECT is indexing not only crack initiation, but also the propensity for crack propagation.
- Tapping mainly compresses the slab. We did not observe any progressive damage in the weak layer prior to fracture, when the weak layer collapses.
- Propagation speeds measured in ECTPs are consistent with previously published results

Broadly speaking, our results are in line with results obtained from PSTs, and are also consistent with mixed mode anticracking [*Heierli et al.*, 2008]. During fracture, weak layers in ECTs compact on the order of several mm, similar to measurements obtained from PSTs [*van Herwijnen et al.,* 2010; *Bair et al.,* 2012]. Measured propagation speeds (on the order of 20 ms^{-1}) are also similar to those for PSTs. The similarities between our results and those with PSTs give us confidence that the fracture mechanics are similar regardless of the triggering mechanism.

However, important differences do exist between the PST and ECT. In a PST, an unstable crack is created by cutting the weak layer with a snow saw until crack propagation occurs while with the ECT the fracture is initiated by tapping on the top of the block. Critical crack lengths with PSTs are typically around 20-40 cm [e.g., *Ross and Jamieson,* 2012], although longer critical crack

lengths are also observed. On the other hand, in an ECT we see no sign of progressive damage in the weak layer. It appears that at the critical loading step, i.e. the final tap, the weak layers fractures over an area directly under the shovel. Thus, ECTs only test crack lengths equal to or less than the shovel width (i.e. about 30 cm). Depending on snow conditions, this crack will either be large enough to propagate or the fracture will arrest.

Our results confirm past observational studies showing that the ECT is a good snowpack test [e.g., *Simenhois and Birkeland,* 2009]. ECT results relate to fracture initiation and propagation, both of which are required for avalanche release. Though this increases our confidence in ECT results for assessing avalanche danger, we continue to caution people that stability tests are only one part of avalanche danger assessments. In the end, a holistic approach utilizing weather, snowpack, and avalanche observations, in addition to stability test results, is necessary for good decision-making in avalanche terrain.

Acknowledgements

We thank Ron Simenhois for reviewing this paper for us. Thanks also go to the Gallatin National Forest Avalanche Center for providing information and logistical support for this work, and to Brad Carpenter, Wes Farnsworth, Eric Knoff, Alex Marienthal, and Robyn Wooldridge for helping out in the field.

References

Bair, E. H., R. Simenhois, K. W. Birkeland, and J. Dozier (2012), A field study on failure of storm snow slab avalanches, *Cold Reg. Sci. Technol.*, *79-80*, 20-28.

Birkeland, K. W., and D. Chabot (In press), Changes in stability test usage by SnowPilot users, *Proceedings of the 2012 International Snow Science Workshop, Anchorage, Alaska (this volume)*.

Crocker, J.C., D.G. Grier, 1996. Methods of digital video microscopy for colloidal studies. Journal of Colloid Interface Science, 179 (1), 298-310.

Gauthier, D., and J. B. Jamieson (2006), Evaluating a prototype field test for weak layer fracture and failure propagation, *Proceedings of the 2006 International Snow Science Workshop, Telluride, Colorado,* 107-116.

Gauthier, D., and J. B. Jamieson (2008), Fracture propagation propensity in relation to snow slab avalanche release: Validating the propagation saw test, *Geophys. Res. Lett.*, *35*(L13501), doi: 10.1029/2008GL034245.

Greene, E. M., et al. (2010), *Snow, Weather and Avalanches: Observation guidelines for avalanche programs in the United States*, 2nd ed., 150 pp., American Avalanche Association, Pagosa Springs, Colorado.

Heierli, J., P. Gumbsch, and M. Zaiser (2008), Anticrack nucleation as triggering mechanism for snow slab avalanches, *Science*, *321*, 240-243.

Johnson, B. C., J. B. Jamieson, and R. R. Stewart (2004), Seismic measurement of fracture speed in a weak snowpack layer, *Cold Reg. Sci. Technol., 40*(1-2), 41-46.

Moner, I., J. Gavalda, M. Bacardit, C. Garcia, and G. Marti (2008), Application of the field stability evaluation methods to the snow conditions of the eastern Pyrenees, *Proceedings of the 2008 International Snow Science Workship, Whistler, B.C.*, 386-392.

Ross, C., and J. B. Jamieson (2008), Comparing fracture propagation tests and relating test results to snowpack characteristics, Proceedings of the 2008 International Snow Science Workshop, Whistler, B.C., 376-385.

Ross, C. and J. B. Jamieson (2012), The propagation saw test: slope scale validation and alternative test methods, *J. Glac., 58*(102), 407-416.

Schweizer, J., A. van Herwijnen, and B. Reuter (2011), Measurements of weak layer fracture energy, *Cold Reg. Sci. Technol.*, *69*(2-3), 139-144.

Simenhois, R., and K. W. Birkeland (2006), The extended column test: A field test for fracture initiation and propagation, *Proceedings of the 2006 International Snow Science Workshop, Telluride, Colorado*, 79-85.

Simenhois, R., and K. W. Birkeland (2009), The Extended Column Test: Test effectiveness, spatial variability, and comparison with the Propagation Saw Test, *Cold Reg. Sci. Technol.*, *59*, 210-216.

Thumert, S., personal communication, Blue River, Canada, 2011.

van Herwijnen, A., and J. Heierli (2009), Measurement of crack-face friction in collapsed weak snow layers, *Geophys. Res. Lett.*, *36*(L23502), doi:10.1029/2009GL040389.

van Herwijnen, A., and J. Heierli (2010), A field method for measuring slab stiffness and weak layer fracture energy, *Proceedings of the 2010 International Snow Science Workshop, Squaw Valley, California*, 232-237.

van Herwijnen, A., and J. B. Jamieson (2005), High speed photography of fractures in weak layers, *Cold Reg. Sci. Technol.*, *43*(1-2), 71-82.

van Herwijnen, A., J. Schweizer, and J. Heierli (2010), Measurement of the deformation field associated with fracture propagation in weak snowpack layers, *Journal of Geophysical Research - Earth Surface*, *115*(F03042).

Winkler, K., and J. Schweizer (2009), Comparison of snow stability tests: Extended column test, rutschblock test and compression test, *Cold Reg. Sci. Technol.*, *59*(2-3), 217-226.